变形晕核中的形状退耦合及转动激发

孙向向　　周善贵

Shape Decoupling Effects and Rotation of Deformed Halo Nuclei

SUN Xiangxiang, ZHOU Shangui

在线阅读 View online: https://doi.org/10.11804/NuclPhysRev.41.2023CNPC56

您可能感兴趣的其他文章

Articles you may be interested in

原子核质量及相关物理量的系统研究

Systematic Study on Nuclear Mass and Related Physical Quantities

原子核物理评论. 2023, 40(2): 141−180　https://doi.org/10.11804/NuclPhysRev.40.2022098

能量密度泛函中不同对关联处理方式对原子核形变描述影响的探讨

Effect of Different Pairing Correlations on the Description of Nuclear Deformations within Energy Density Functional Framework

原子核物理评论. 2020, 37(1): 26−33　https://doi.org/10.11804/NuclPhysRev.37.2020006

复动量表象方法对奇特核中晕现象的研究

Study on Halo Phenomenon in Exotic Nuclei by Complex Momentum Representation Method

原子核物理评论. 2020, 37(3): 574−579　https://doi.org/10.11804/NuclPhysRev.37.2019CNPC07

超越平均场模型对Ba同位素链八极形状演化研究

Beyond−mean−field Study of Octupole Shape Evolution in Neutron−deficient Ba Isotopes

原子核物理评论. 2019, 36(2): 144−150　https://doi.org/10.11804/NuclPhysRev.36.02.144

基于相对论Hartree−Fock理论的原子核壳结构性质研究

Nuclear Shell Structure Properties Described by Relativistic Hartree−Fock Theory

原子核物理评论. 2020, 37(3): 478−491　https://doi.org/10.11804/NuclPhysRev.37.2019CNPC61

原子核第一激发能的统计规律

Statistical Features of the First Excitation Energy of Nuclei

原子核物理评论. 2019, 36(4): 408−413　https://doi.org/10.11804/NuclPhysRev.36.04.408

Editors' Suggestion

Shape Decoupling Effects and Rotation of Deformed Halo Nuclei

SUN Xiangxiang[1,2], ZHOU Shangui[1,2,3,4,†]

(*1. School of Nuclear Science and Technology, University of Chinese Academy of Sciences, Beijing 100049, China*;
2. CAS Key Laboratory of Theoretical Physics, Institute of Theoretical Physics,
Chinese Academy of Sciences, Beijing 100190, China;
3. School of Physical Sciences, University of Chinese Academy of Sciences, Beijing 100049, China;
4. Peng Huanwu Collaborative Center for Research and Education, Beihang University, Beijing 100191, China)

Abstract: With the development of radioactive-ion-beam facilities, many exotic phenomena have been discovered or predicted in the nuclei far from the β stability line, including cluster structure, shell structure, deformed halo, and shape decoupling effects. The study of exotic nuclear phenomena is at the frontier of nuclear physics nowadays. The covariant density functional theory (CDFT) is one of the most successful microscopic models in describing the structure of nuclei in almost the whole nuclear chart. Within the framework of CDFT, toward a proper treatment of deformation and weak binding, the deformed relativistic Hartree-Bogoliubov theory in continuum (DRHBc) has been developed. In this contribution, we review the applications and extensions of the DRHBc theory to the study of exotic nuclei. The DRHBc theory has been used to investigate the deformed halos in B, C, Ne, Na, and Mg isotopes and the theoretical descriptions are reasonably consistent with available data. A DRHBc Mass Table Collaboration has been founded, aiming at a high precision nuclear mass table with deformation and continuum effects included, which is underway. By implementing the angular momentum projection based on the DRHBc theory, the rotational excitations of deformed halos have been investigated and it is shown that the deformed halos and shape decoupling effects also exist in the low-lying rotational excitation states of deformed halo nuclei.

Key words: exotic nuclei; deformed halo; shape decoupling effect; nuclear mass; rotational excitation; density functional theory

0 Introduction

In nature, there are less than three hundred stable or long-lived nuclides, which form the β-stability valley of the nuclear chart[1]. About three thousand nuclides are found to be unstable and their properties are less known compared with those stable ones. With the development of radioactive-ion-beam facilities, more and more unstable nuclei are produced, which extends the limit of nuclear existence. Up to now, the position of the proton drip line has been determined up to $Z = 93$[2] but the neutron drip line is only known for isotopes with $Z \leqslant 10$[3]. Exploring the boundaries of nuclear landscape and the properties of exotic nuclei is at the forefront of nuclear physics nowadays.

Many exotic nuclear phenomena have been predicted or observed[4−15]. The most important characteristic of exotic nuclei is their weak binding. For unstable nuclei, especially those close to drip lines, the nucleon Fermi surface is close to the threshold of particle emission [Fig. 1(a)] and nucleon separation energies are close to zero [Fig. 1(b)]. Therefore the coupling to scattering states becomes more important, making exotic nuclei open quantum systems[7, 16]. Once the valence nucleons in weakly bound nuclei occupy low orbital angular momentum orbitals, whose wave functions can extend far away from the center of the nucleus due to the low centrifugal barrier, in which case the nuclear halo may appear [Fig. 1(c)][7, 11, 17]. The phenomenological picture of halo nucleus is a dense core surrounded by very low-density pure neutron (proton) matter, in which pair condensate or strong di-neutron correlations may oc-

Biography: SUN Xiangxiang(1993–), male, post-doctor at Institute for Advanced Simulation, Forschungszentrum Jülich, D-52425 Jülich, Germany, working on nuclear structure and reaction; E-mail: x.sun@fz-juelich.de

† **Corresponding author:** ZHOU Shangui, E-mail: sgzhou@itp.ac.cn

cur[18−20]. Most open shell nuclei are deformed[21] and halo can also appear in a deformed nucleus[22], such as ^{31}Ne and ^{37}Mg[23−24]. In deformed halo nuclei, it has been predicted that the core and halo may have different shapes, leading to shape decoupling effects [Fig. 1(e) and (f)][12, 22, 25]. The spin-orbit splitting changes when going from the β-stability line to the drip lines because the nuclear surface could be more diffuse [Fig. 1(g)][26]. This results in the shell evolution in exotic nuclei and changes of nuclear magicit-

ies[8]. Beyond the drip lines, nuclei are unbound with respect to nucleon(s) emission, which implies some new radio-activities of which mostly discussed are one- or two-proton radioactivities [Fig. 1(h)][27−29]. Cluster effects[14, 30] appear in some stable nuclei if they are excited to be close to certain thresholds and have gained general interest for both experimental and theoretical sides, a typical example being the α-cluster in the Hoyle states in ^{12}C. In exotic nuclei, the ground states are mainly dominated by cluster configurations.
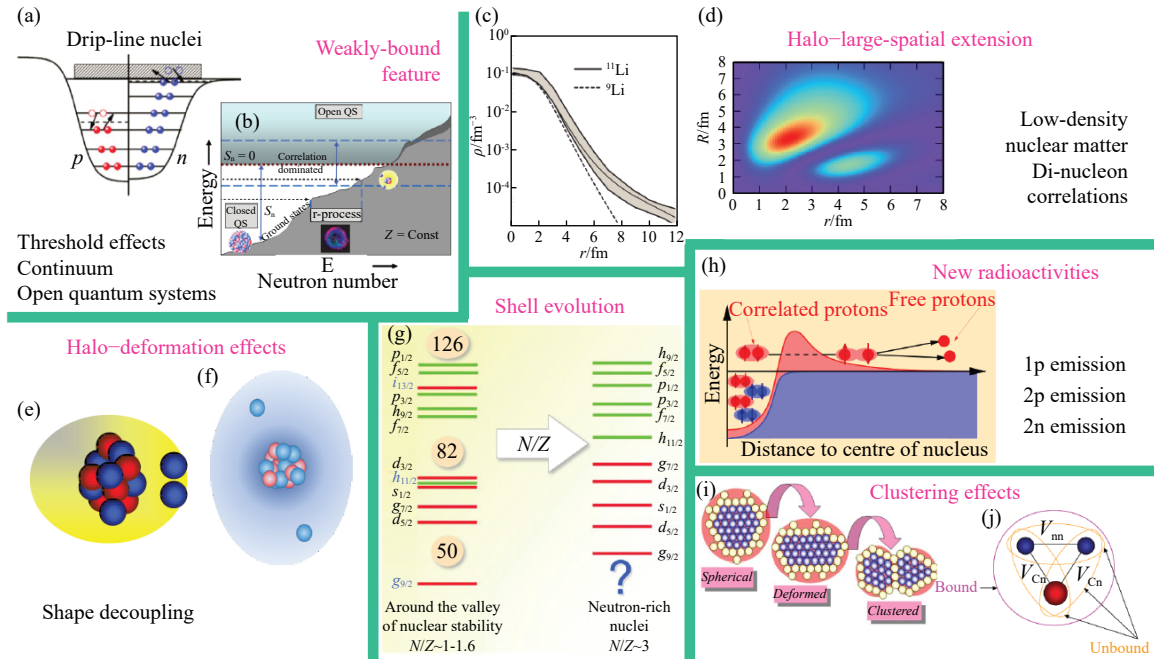

Fig. 1　Physics in exotic nuclear structure[4]. (color online)

The covariant density functional theory (CDFT) has become a powerful tool for the study of stable and exotic nuclei over almost the whole nuclear chart with universal density functionals[7, 12−13, 31−35]. The coupling between bound single-particle states and continuum which plays an important role in exotic nuclei has been properly considered by solving the Dirac Hartree-Bogoliubov equation in coordinate space or r-space Woods-Saxon (WS) basis. Along this line, several approaches have been established for spherical and deformed nuclei. The relativistic continuum Hartree-Bogoliubov (RCHB)[17, 36−38] and relativistic Hartree-Fock-Bogoliubov (HFB) theories[39] have been developed for spherical halo nuclei, such as the halo in ^{11}Li[17] and the prediction of giant halos in Ca isotopes[38]. With a proper treatment of deformation and pairing-induced continuum, the deformed relativistic Hartree-Bogoliubov theory in continuum (DRHBc theory) has been developed aiming at a self-consistent description of deformed halo nuclei[22]. In recent years, this theory has been widely used to study deformed halos in B, C, Ne, Na, and Mg isotopes[22, 25, 40−46] and its extension with angular momentum projection (AMP) has been used to explore

the rotational excitation of deformed halos[47−48]. In addition, the construction of the DRHBc nuclear mass table is in progress[49−51] and many interesting nuclear structures have been studied. In this contribution, we review the applications and extensions of the DRHBc theory to the study of exotic nuclei and nuclear mass table.

This article is organized as follows. In Section 1, we present the main formulas of the DRHBc theory and AMP. We summarize the application of the DRHBc theory to deformed halo in Section 2 and DRHBc mass table in Section 3. The study of rotational properties of deformed halo is shown in Section 4. Finally, we give a summary and perspective in Section 5.

1　The DRHBc theory and angular momentum projection

The starting point of the DRHBc theory is a Lagrangian density where nucleons are described as Dirac spinors which interact via the exchange of effective mesons (σ, ω, ρ) and the photon

$$\mathcal{L} = \bar{\psi}(\mathrm{i}\partial\!\!\!/ - M)\psi + \frac{1}{2}\partial_\mu\sigma\partial^\mu\sigma - U(\sigma) - g_\sigma\bar{\psi}\sigma\psi -$$

$$\frac{1}{4}\Omega_{\mu\nu}\Omega^{\mu\nu} + \frac{1}{2}m_\omega^2\omega_\mu\omega^\mu - g_\omega\bar{\psi}\omega\!\!\!/\psi -$$

$$\frac{1}{4}\boldsymbol{R}_{\mu\nu}\boldsymbol{R}^{\mu\nu} + \frac{1}{2}m_\rho^2\vec{\rho}_\mu\vec{\rho}^\mu - g_\rho\bar{\psi}\vec{\rho}\!\!\!/\vec{\tau}\psi -$$

$$\frac{1}{4}F_{\mu\nu}F^{\mu\nu} - e\bar{\psi}\frac{1-\tau_3}{2}A\!\!\!/\psi, \tag{1}$$

where M is the nucleon mass and $m_\sigma, m_\omega, m_\rho$, and g_σ, g_ω, g_ρ are masses and coupling constants of the respective mesons. U is the nonlinear self-coupling for the scalar meson.

The detailed formulas for the DRHBc theory can be found in Zhou *et al.*[22], Li *et al.*[40]. In the DRHBc theory, by using the Bogoliubov transformation, the mean-field (MF) and pairing correlations are treated self-consistently[36, 52]. Here we give briefly the main formulas for the convenience of discussions in the following sections. The relativistic Hartree-Bogoliubov (RHB) equation[53] for nucleons reads,

$$\begin{pmatrix} h_D - \lambda_\tau & \Delta \\ -\Delta^* & -h_D^* + \lambda_\tau \end{pmatrix}\begin{pmatrix} U_k \\ V_k \end{pmatrix} = E_k\begin{pmatrix} U_k \\ V_k \end{pmatrix}, \tag{2}$$

which is solved in a spherical Dirac Woods-Saxon (WS) basis[54]. E_k is the quasi particle energy, λ_τ ($\tau = \mathrm{n, p}$) is the chemical potential, and U_k and V_k are quasi particle wave functions. h_D is the Dirac Hamiltonian[31, 55],

$$h_D = \boldsymbol{\alpha} \cdot \boldsymbol{p} + V(\boldsymbol{r}) + \beta[M + S(\boldsymbol{r})], \tag{3}$$

where $S(\boldsymbol{r})$ and $V(\boldsymbol{r})$ are scalar and vector potentials. The pairing potential reads

$$\Delta(\boldsymbol{r}_1, \boldsymbol{r}_2) = V^{\mathrm{pp}}(\boldsymbol{r}_1, \boldsymbol{r}_2)\kappa(\boldsymbol{r}_1, \boldsymbol{r}_2), \tag{4}$$

where we use a density dependent zero-range force in the particle-particle channel,

$$V^{\mathrm{pp}}(\boldsymbol{r}_1, \boldsymbol{r}_2) = \frac{1}{2}V_0(1 - P^\sigma)\delta(\boldsymbol{r}_1, \boldsymbol{r}_2)\left(1 - \frac{\rho(\boldsymbol{r}_1)}{\rho_{\mathrm{sat}}}\right), \tag{5}$$

and $\kappa(\boldsymbol{r}_1, \boldsymbol{r}_2)$ is the pairing tensor[56].

We would like to mention that for a spherical nucleus Eq. (2) can be directly solved in coordinate space[17], as has been done in the RCHB theory which has been used to study spherical halo nuclei[17, 38] and to construct RCHB mass table [57]. It is numerically much more complicated to solve the deformed RHB equation in coordinate space. One can solve it in the WS basis[54]. Thus, to get the solution of deformed RHB equation, the integrodifferential equations turns into a matrix diagonalization problem in the WS basis[40]. The main advantage of the WS basis is that it can guarantee the asymptotic behavior of the wave function for a weakly bound system[54] such that it is suitable for halo nuclei. The WS basis has also been widely used in other density functional theory calculations[50, 58−63].

For axially deformed nuclei with spatial reflection symmetry, we expand densities and potentials in terms of Legendre polynomials,

$$f(\boldsymbol{r}) = \sum_\lambda f_\lambda(r)P_\lambda(\cos\theta), \quad \lambda = 0, 2, 4, \cdots, \tag{6}$$

with

$$f_\lambda(r) = \frac{2\lambda + 1}{4\pi}\int \mathrm{d}\Omega f(\boldsymbol{r})P_\lambda(\cos\theta). \tag{7}$$

When the maximum truncation in Eq. (6) is taken to be zero, the solution is equal to that of the RCHB theory. If one wants to extend the DRHBc theory to axially deformed systems with spatial reflection asymmetry, odd λ should be included. One can also use the spherical harmonic expansion for triaxially deformed systems[64−65] and for AMP calculations[47].

To study the rotational excitation of deformed weakly bound nuclei, the AMP has been implemented based on the DRHBc theory[47], in which the projected wave function is expanded in terms of the Dirac WS basis, similar to what has been done for the MF wave function in the DRHBc theory. A low-lying rotational state $|JM\rangle$ with the angular momentum J and its projection M along the z axis in laboratory frame is constructed by performing the AMP on the intrinsic wave function $|\Phi(\beta_2)\rangle$ obtained from DRHBc calculations with a certain quadrupole deformation parameter β_2

$$|\Psi^{JM}\rangle = f^J\hat{P}_{M0}^J|\Phi(\beta_2)\rangle, \tag{8}$$

with a normalization factor f^J and projection operator $\hat{P}_{M0}^J$ written in terms of an integral over the Euler angles[56]. The energy E^J and f^J can be obtained by solving the Hill-Wheeler equation[56]. For axially symmetric nuclei the solution is simplified as[66]

$$E^J = \frac{\langle\Phi(\beta_2)|\hat{H}\hat{P}_{00}^J|\Phi(\beta_2)\rangle}{\langle\Phi(\beta_2)|\hat{P}_{00}^J|\Phi(\beta_2)\rangle},$$
$$f^J = \frac{1}{\sqrt{\langle\Phi(\beta_2)|\hat{P}_{00}^J|\Phi(\beta_2)\rangle}}. \tag{9}$$

The DRHBc theory provides a self-consistent description of a deformed halo nucleus in the intrinsic frame without a priori decomposition of the core and halo, which are determined by analyzing the structure of single-particle-levels (SPLs) after getting the ground state wave functions[12, 22]. By checking the core and halo density distributions, shape decoupling effects of deformed halos have been predicted in the MF level[22]. To examine how the core and halo behave in rotational states, one can calculate the one-body density of an excited state in coordinate space[67]

$$\rho^J(\boldsymbol{r}) = \left\langle \Psi^{JM}\left|\sum_i \delta(\boldsymbol{r} - \boldsymbol{r}_i)\right|\Psi^{JM}\right\rangle, \tag{10}$$

where the index i represents all occupied single-particle states of neutrons and protons.

Deformed halos and shape decoupling effects are attributed to the intrinsic structure of valence levels[22]. The configuration of the valence nucleon(s) is obtained by calculating the probability amplitude of spherical components of valence levels in the DRHBc+AMP approach. The Dirac WS basis[54] consists of spherical basis states labeled by $|nlj\rangle$ with the radial quantum number n, the orbital angular momentum l of the large component of the Dirac spinor, and the total angular momentum j. For each excited state, the probability amplitude of $|nlj\rangle$ is calculated as[68]

$$N_{nlj}^J = \frac{\langle \Phi(\beta_2)|\hat{N}_{nlj}\hat{P}_{00}^J|\Phi(\beta_2)\rangle}{\langle \Phi(\beta_2)|\hat{P}_{00}^J|\Phi(\beta_2)\rangle}, \tag{11}$$

where $\hat{N}_{nlj} = \sum_m c_{nljm}^\dagger c_{njlm}$ with m being the projection of total angular momentum on the symmetry axis.

2　Halos in deformed nuclei

Nuclear halo is characterized by weak binding and large spatial extension due to the considerable occupation of low-l (s- or p-wave) orbitals by valence nucleon(s) close to the threshold of the particle emission[6, 10, 17, 36−37, 69−70]. The various shapes of atomic nuclei originate from different quantum correlations. For example, the quadrupole deformation (ellipsoidal shape) is related to the Y_{20} correlation and the Y_{30} correlation for octupole deformation (pear-shaped). For a weakly bound nucleus in the light mass region, if the configuration of valence nucleons contains the mixing of sd or pf orbtials, a deformed halo might be developed. In neutron-rich B, C, Ne, Na, and Mg isotopes, such conditions can be satisfied such that deformed halos are formed. The DRHBc theory has been used to study the ground-state properties, including deformations, matter radii, density profiles, and single-particle levels, of deformed halo nuclei in these isotopic chains. In this section, first, we give a typical example to show how the halo forms in a deformed weakly bound nucleus and then we summarise the application of the DRHBc theory on deformed halos and the comparison with the available experimental information.

The first application of the DRHBc theory is to study the deformed halo structures in the magnesium isotopic chain. With the density functional NL3[71], the DRHBc calculations predicted that ^{46}Mg is the neutron drip line nucleus[22] and ^{44}Mg is a deformed halo nucleus. The two-neutron separation energy S_{2n} of ^{44}Mg is very small, only 0.44 MeV, and the quadrupole deformation parameter β_2 is 0.32, meaning that the ground state has a prolate shape. Fig. 2(a) shows the proton and neutron two-dimensional density distribution of ^{44}Mg. Since ^{44}Mg is an extremely weakly bound neutron-rich nucleus, the neutron density is more spatially extended than the proton density. In the MF ap-

proach, the configuration and formation mechanism of the halo nucleus can be obtained by analyzing the structure of the valence orbitals. In Fig. 3, the neutron SPLs of ^{44}Mg in the canonical basis near the neutron Fermi level (λ_n) is shown. Near the neutron Fermi level, the valence neutrons occupy weakly bound $\frac{3}{2}^-$, $\frac{1}{2}^-$ levels, and some orbitals in the continuum. There are p-wave components in the levels $n = 3, 4, 6$, and the occupation number of the p-wave orbitals is about 2, which leads to the halo structure of this nucleus.
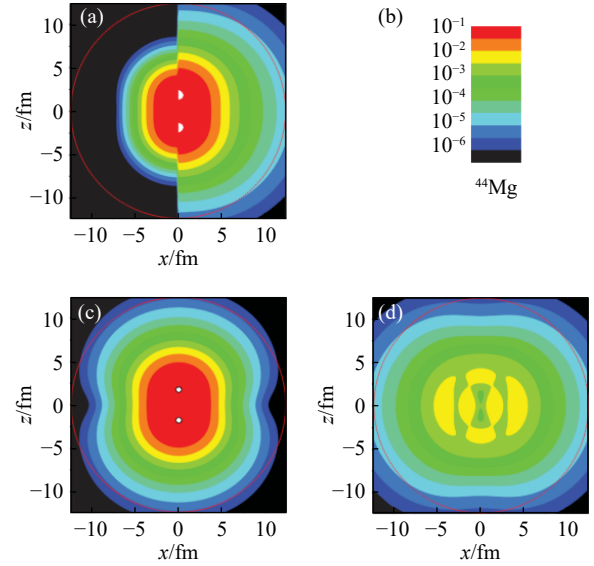

Fig. 2　Density distributions of ^{44}Mg with the z-axis as the symmetry axis: (a) The proton ($x < 0$) and the neutron ($x > 0$) densities, (b) the density of the neutron core, and (c) the density of the neutron halo. In each plot, a dotted circle is drawn to guide the eye[22]. (color online)
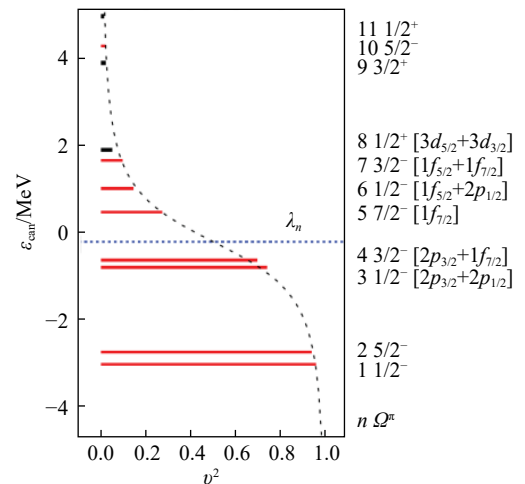

Fig. 3　Single neutron levels with the quantum numbers Ω^π around the chemical potential (dotted line) in the canonical basis for ^{44}Mg versus the occupation probability v^2. The order n, Ω^π, and the main DWS components for orbitals close to the threshold are also given. The dashed line corresponds to the BCS formula with an average pairing gap[22]. (color online)

In the DRHBc theory description of magnesium isotopes, ^{42}Mg is a deformed two-neutron halo nucleus[40], and its halo structure is caused by the *p*-wave dominated valence neutrons. However, the heaviest observed magnesium isotope is ^{40}Mg up to now[72]. Therefore the existence of deformed halos in $^{42, 44}$Mg still requires further experimental confirmation. Whether ^{40}Mg is a deformed halo nucleus remains an open question. The DRHBc theory predicts that ^{40}Mg is not a deformed halo nucleus. It should be noted that the triaxial deformation plays a role in the description of ^{40}Mg[73] and the influence of triaxial deformation on single particle structure should be investigated in future. In Mg isotopes, a single-neutron halo has already been observed experimentally in ^{37}Mg[24]. Considering the blocking effect, the DRHBc calculations with different density functionals have shown that ^{37}Mg is a deformed one-neutron halo nucleus[46] with *p*-wave.

For the B isotopic chain, the DRHBc theory has predicted the existence of deformed neutron halos in $^{17, 19}$B[43−44] with the valence neutrons occupying the *s*-wave orbital. The *s*-wave component of the two valence neutrons in ^{17}B obtained from quasi-free neutron knockout reactions is only 9(2)%[43]. The deformation of ^{17}B has been studied in 2005[74] and the quadrupole deformation parameter of neutrons is about 0.6[75]. The DRHBc theory predicts that ^{17}B is well deformed with the *s*-wave component of 14% and the calculated neutron separation energy and radius are consistent with experimental data. The measurements of the $B(E1)$ excitation in ^{19}B by using Coulomb breakup reactions confirmed the presence of a neutron halo[76]. Assuming the two-neutron separation energy being 0.5 MeV, a three-body model suggests that ^{19}B is a two-neutron halo nucleus caused by the *s*-wave with the percentage of 35%. The antisymmetrized molecular dynamics and relativistic mean-field calculations have predicted that ^{19}B is deformed[77−79]. The DRHBc calculations show that the halo in ^{19}B is crucially related to the deformation effects and the valence neutrons are mainly dominated by *s*- and *d*-waves with the *s*-wave percentage of 36%. Furthermore, the two-neutron halos in $^{17, 19}$B exhibit shape decoupling effects, prolate cores and oblate halos. The neutron drip line of B

isotopic chain is located at ^{19}B and experimentalists have observed ^{20}B and ^{21}B as resonance states[80], which might be dominated by the channels ^{19}B+n and ^{19}B+2n, respectively. Therefore it will be very interesting to study the structure of the resonant states in $^{20, 21}$B based on a proper description of halo structure in ^{19}B.

For the C isotopic chain, the DRHBc theory predicts that ^{15}C and ^{22}C are deformed halo nuclei[25, 42]. The ground state of ^{15}C has a prolate shape and the valence neutron is partially occupied with *s*-wave, leading to the appearance of a halo. The neutron core is nearly spherical while the neutron halo has an elongated shape, demonstrating the shape decoupling effect. Recent calculations using time-dependent density functional theory have shown that the deformed halo structure of ^{15}C enhances fusion cross-sections below the Coulomb barrier in the fusion reaction with ^{232}Th[81]. For ^{22}C, the halo configuration of this nucleus is not completely determined up to now experimentally. The measurement in 2010[82] shown that the matter radius extracted from the cross section is 5.4 fm, indicating a huge halo. The two-neutron removal reaction in 2012[83] supported that the valence neutrons are dominated by *s*-wave. But the following experimental work[84] shows a matter radius of (3.44 ± 0.08) fm. The theoretical descriptions of this nucleus vary from model to model[60, 85−97]. The DRHBc theory calculations show that the ground state of ^{22}C has an oblate shape and predict a "shrunk halo" due to the amplitude of *s*-wave in valence neutrons being 25%, which is smaller than the other theoretical predictions[25]. In addition, this work[25] also demonstrates that various exotic nuclear phenomena, including deformed halos, changes of shell-closure due to the inversion of SPLs, and shape decoupling effects coexist in this single nucleus ^{22}C. As for ^{19}C, the DRHBc calculations show an oblate shape for its ground state without a neutron halo. The calculated ground state spin-parity, $\frac{3}{2}^+$, does not agree with the experiment $\frac{1}{2}^+$. However, in the DRHBc calculations, an excited state of ^{19}C with prolate shape (referred as ^{19}C*) has the spin-parity of $\frac{1}{2}^+$ and exhibits a deformed one-neutron halo.

We summarize the DRHBc predictions for *s*-wave halo in Table 1 and some available experimental informa-

Table 1 The quadrupole deformation parameter β_2, two- or one- neutron separation energy $S_{2n}(S_n)$, root-mean-square matter radius R_m, and the amplitude of *s*-wave components of the halo nuclei in born and carbon isotopes from the DRHBc calculations. Available experimental values are included for comparison. The experimental data of neutron-separation energies are taken from AME2020[98].

Nuclei	β_2	S_{2n} (S_n)/MeV		R_m/fm		Percentage of *s*-wave	Shape decoupling
	DRHBc	DRHBc	Exp.	DRHBc	Exp.	DRHBc	
^{17}B	0.52	1.78	1.38(21)	3.03	3.00(6)[99]	14%	prolate core with oblate halo
^{19}B	0.36	0.22	0.089(56)	3.27	3.11(13) [99]	36%	prolate core with oblate halo
^{15}C	0.26	1.22	1.2181(8)	2.64	2.54(4) [100]	36%	spherical core with prolate halo
^{19}C*	0.37	0.04	0.563 3(915)	3.05	3.16(7)[100]	66%	prolate core with oblate halo
^{22}C	−0.26	0.40	0.035(20)	3.25	3.44(8)[84]	25%	oblate core with prolate halo

tion is also given for comparison. Besides the studies mentioned above, the DRHBc theory is also applied to the newly observed Na isotopes ^{39}Na and has predicted that ^{39,41}Na have deformed halos[45]. The self-consistent description of deformed halos using the DRHBc theory is also combined with reaction models to examine the reaction observables, such as interaction cross section and parallel momentum distributions in breakup reaction[101]. With the Fock terms considered, the deformed relativistic Hartree-Fock-Bogoliubov theory has been developed recently[61] and it has been applied to the halo in ^{11}Be[102]. It should be noted that the predictions of deformed halos can also be made by using non-relativistic MF models[103−106] and an "egg-like" halo has been predicted[103]. Other methods, such as Green's function method[107−108], complex scaling method[109], and the analytical continuation of the coupling constant[110] based on self-consistent MF calculation are also used to investigate the halo structures in deformed nuclei.

3   The DRHBc Mass Table Collaboration

Nuclear mass, as one of the most fundamental quantities for the atomic nucleus, is very important for nuclear physics, astrophysics and cosmology. It is the key to understanding the interaction between nucleons, the evolution of shell structures, and the limit of nuclear existence. It also provides the basic information for nuclear reactions and the necessary inputs to study the origin of elements. Up to now, many nuclear models have been used to establish nuclear mass tables, such as finite-range droplet model (FRDM)[111−112], Weizsäcker-Skyrme 4 (WS4) model[113−114], and HFB-27* model[115]. The DRHBc Mass Table Collaboration consists of more than 20 institutions from China, Korea, and Japan, including Peking University, Anhui University, Beihang University, Huzhou Normal University, Institute for Basic Science, Institute of Modern Physics, Chinese Academy of Sciences, Institute of Theoretical Physics, Chinese Academy of Sciences, Nanjing University of Aeronautics and Astronautics, Pusan National University, Sichuan Normal University, Soongsil University, Southwest University, Sungkywan University, the University of Hong Kong, Zhengzhou University, Guizhou Minzu University, the University of Tokyo, Institute of Nuclear Physics and Chemistry, China Academy of Engineering Physics, Jiangnan University, Lanzhou University, Nankai University, Sun Yat-sen University, University of Chinese Academy of Sciences, and so on[116], aiming to the bulk properties of all bound nuclei with $Z \geqslant 8$ based on the systematic calculations of all the nuclei in the nuclear chart. After careful checking for the numerical details of the DRHBc theory with density functional PC-PK1[41], the nuclear mass table for all the even-even nuclei has been fin-

ished[50]. It has been shown that with the effects of deformation and continuum included simultaneously, 2583 even–even nuclei are predicted to be bound and the root-mean-square deviation from the 637 mass data is 1.518 MeV, providing one of the best microscopic descriptions for nuclear masses. For calculating odd-A or odd-odd nuclei, treating the blocking effects automatically has been achieved within the DRHBc theory[51], which is suitable for large-scale DRHBc calculations. The mass table for all the even-Z odd-N nuclei has been finished[117] and the next step aims to odd-Z nuclei.

Many interesting exotic nuclear structures have also been studied based on the global DRHBc calculations. The effect of deformation on the position of the drip lines for $8 \leqslant Z \leqslant 20$ has been studied[118]. The dependence on the multipole expansion of the potentials and densities in DRHBc has been carefully checked[119]. Considering the deformation effects, the pairing correlations, and the continuum effects, possible stability against multineutron emission beyond the two-neutron drip line have been explored by the DRHBc theory[120−123]. The calculations of Hf, W, Os, Pt, and Hg even-even isotopes have predicted some candidates with both bubble structure and shape coexistence[124]. Possible shape coexistence in Pb isotopes[125] and prolate-shape dominance in atomic nuclei[126] are also investigated. Additionally, beyond-mean-field dynamical correlations for nuclear mass have been considered[127] and the finite amplitude method has been developed[128].

4   Angular momentum projection: Rotating deformed halos

The beyond-mean-field approaches including AMP have been widely used to study nuclear collective motions[13, 34, 129] and also for exotic nuclear structure, for instance, the shape coexistence[130−131], shell evolution[132], low-lying excitation of hypernuclei[133−136], excitation of triaxially deformed nuclei[137−142], nuclear octupole excitation[143−145], the structure and fission of superheavy nuclei[146−148], and exotic shapes[149−152]. One of the motivations for developing AMP based on the DRHBc theory is to explore how the shape decoupling effects behave in the rotational states and to predict some signals that can be detected. The MF studies on halo nuclei have shown that the deformation of halo nuclei is connected to the evolution of shells[25, 44]. It is well-established that nuclear shapes and shell closures can be reflected by nuclear collective excitation spectra. The implementation of AMP based on the DRHBc theory can be also used to study the properties of collective excitations in deformed halo nuclei[47], which can provide insight into halo configurations for a better understanding of the mechanism for deformation-driven halos. In this section, we take the rotation

of the two-neutron halo nucleus as an example to show the properties of deformed halos in excited states.

Neutron-rich Mg isotopes ^{40}Mg, ^{42}Mg, and ^{44}Mg are well deformed with $\beta_2 = 0.46$, 0.38, and 0.31, respectively based in the DRHBc calculations with PC-PK1[153]. The ground state of ^{42}Mg has a deformed halo which is caused by the considerable occupation of p-wave components in weakly bound valence neutron levels[40, 48]. According to the structure of SPLs, the density of a halo nucleus can be divided into the halo part contributed from valence nucleons and the core part from the other tightly bound orbitals. In the first row of Fig. 4, we show the densities of the whole nucleus, all neutrons, neutron core, and neutron halo in the *xz* plane from left to right for ^{42}Mg. One can see that the core has a prolate shape while the halo is slightly oblate, which means that ^{42}Mg is a deformed halo nucleus with shape decoupling effects.
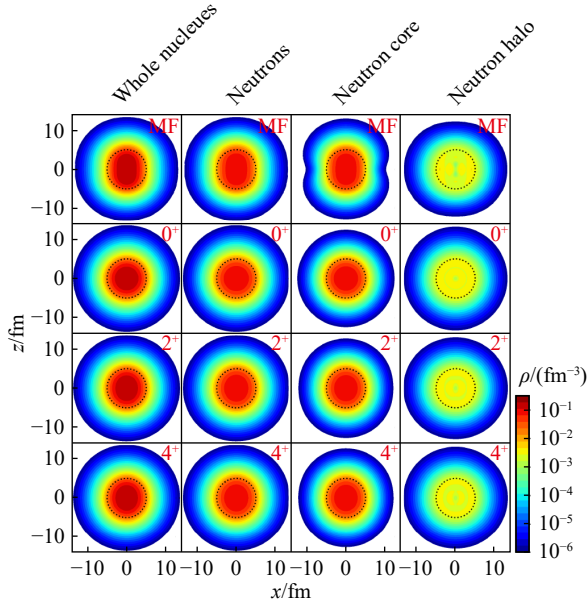

Fig. 4   Densities for the whole nucleus, all neutrons, the neutron core, and neutron halo of ^{42}Mg in the MF ground state and projected 0^+, 2^+, and 4^+ states (with M=0)[48]. Black dotted circles are given to guide the eye. (color online)

Using the intrinsic wave functions of ^{42}Mg obtained from DRHBc calculations, one can get the excited-state wave functions by using AMP and subsequently investigate their properties. The results demonstrate that the excitation spectrum based on the deformed ground-state wave function of ^{42}Mg conforms to the feature of nuclear rotational excitations, wherein the excitation energy linearly correlates with the square of the angular momentum. By computing the expectation value of the one-body density operator in the projected wave functions, we can determine the density distribution of the excited states. The partitioning of the neutron core and halo introduced in the intrinsic frame remains in the projected excited states for the one-

body density operator. Fig. 4 also includes the density distributions of the whole nucleus, neutron halo, neutron core, and neutrons for the 0^+, 2^+, and 4^+ states. It can be seen that the halo structure persists in the excited states. For the 0^+ state, the nuclear density distribution is spherical, resulting in spherical density distributions for the neutron halo and core such that there are no shape decoupling effects. In the 2^+ and 4^+ states, we find that the core and halo have different shapes, which means that the shape decoupling effects are preserved. To understand this, we calculated the configuration of each rotational excited states, see Fig. 5. It is found that the configurations of valence neutrons almost do not change with respect to the angular momentum. Consequently, the presence of deformed halo structures and shape decoupling effects in the intrinsic frame persists in the low-lying rotational states. This prediction awaits experimental verification. In addition, in AMP calculations we still did not find the clue to detect shape decoupling effects and it is still an open question what kind of observables are closely related to this exotic structure. We hope that one can find some signals in future precise measurement on the density distribution and the scattering of hadronic probes.
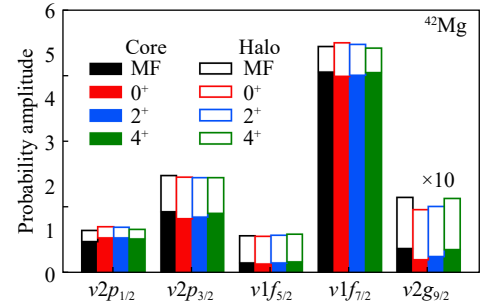

Fig. 5   Probability amplitudes of *p*-, *f*-, and *g*-wave components contributed to the halo and core of the MF ground state and each collective state for ^{42}Mg[48]. The probability amplitude of $\nu 2g_{9/2}$ is multiplied by 10. (color online)

5   Summary and perspective

In this contribution, we have summarized the applications of the DRHBc theory and its extensions. This theory has been used to describe deformed halo structures in B, C, Ne, Na, and Mg isotopes. The DRHBc mass table collaboration has been established and the DRHBc nuclear mass table is under construction, meanwhile different groups in this collaboration also use the DRHBc theory to study exotic nuclear structures in the mass regions of which they are in charge. The AMP based on the DRHBc theory has been developed to study the rotational excitations of deformed halo nuclei.

The nature of the halo nuclei is related to their shapes. At present, based on the DRHBc theory, the influence of

reflection-asymmetry deformation on halo structure has not been considered. So it is necessary to extend the DRHBc theory in this direction. Since hyperons do not need to obey the Pauli principle of nucleons, they can be utilized as "probes" to detect the properties of atomic nuclei, for example, to explore the effect of hyperons on the properties of deformed halo nuclei. This requires to consider the hyperon degrees of freedom within the framework of the DRHBc theory. In beyond-mean-field calculations based on the DRHBc theory, only the AMP has been included. The inclusion of the particle number projection to treat the fluctuation of particle number and the generator coordinates method to deal with the quantum fluctuation of collective degrees of freedom are also future tasks for a fully self-consistent description of the deformed halo from ground states to excited states.

References:

[1]   THOENNESSEN M. Rep Prog Phys, 2013, 76(5): 056301.

[2]   ZHANG Z Y, GAN Z G, YANG H B, et al. Phys Rev Lett, 2019, 122(19): 192503.

[3]   AHN D S, FUKUDA N, GEISSEL H, et al. Phys Rev Lett, 2019, 123(21): 212501.

[4]   ZHOU S G. PoS, 2017, INPC2016: 373.

[5]   ZHUKOV M, DANILIN B, FEDOROV D, et al. Phys Rep, 1993, 231(4): 151.

[6]   JENSEN A S, RIISAGER K, FEDOROV D V, et al. Rev Mod Phys, 2004, 76(1): 215.

[7]   MENG J, TOKI H, ZHOU S G, et al. Prog Part Nucl Phys, 2006, 57(2): 470.

[8]   SORLIN O, PORQUET M G. Prog Part Nucl Phys, 2008, 61(2): 602.

[9]   FREDERICO T, DELFINO A, TOMIO L, et al. Prog Part Nucl Phys, 2012, 67(4): 939.

[10] RIISAGER K. Phys Scr, 2013, 2013(T152): 014001.

[11] TANIHATA I, SAVAJOLS H, KANUNGO R. Prog Part Nucl Phys, 2013, 68: 215.

[12] MENG J, ZHOU S G. J Phys G: Nucl Part Phys, 2015, 42(9): 093101.

[13] MENG J. Relativistic Density Functional for Nuclear Structure[M/OL]. World Scientific, 2016. DOI: 10.1142/9872.

[14] FREER M, HORIUCHI H, KANADA-EN'YO Y, et al. Rev Mod Phys, 2018, 90(3): 035004.

[15] OTSUKA T, GADE A, SORLIN O, et al. Rev Mod Phys, 2020, 92(1): 015002.

[16] MICHEL N, NAZAREWICZ W, OKOŁOWICZ J, et al. J Phys G: Nucl Part Phys, 2010, 37(6): 064042.

[17] MENG J, RING P. Phys Rev Lett, 1996, 77(19): 3963.

[18] HAGINO K, SAGAWA H, CARBONELL J, et al. Phys Rev Lett, 2007, 99(2): 022506.

[19] MATSUO M. Phys Rev C, 2006, 73(4): 044309.

[20] SUN B Y, TOKI H, MENG J. Phys Lett B, 2010, 683(2): 134.

[21] ZHOU S G. Phys Scr, 2016, 91(6): 063008.

[22] ZHOU S G, MENG J, RING P, et al. Phys Rev C, 2010, 82(1): 011301(R).

[23] NAKAMURA T, KOBAYASHI N, KONDO Y, et al. Phys Rev Lett, 2014, 112(14): 142501.

[24] KOBAYASHI N, NAKAMURA T, KONDO Y, et al. Phys Rev Lett, 2014, 112(24): 242501.

[25] SUN X X, ZHAO J, ZHOU S G. Phys Lett B, 2018, 785: 530.

[26] DOBACZEWSKI J, MICHEL N, NAZAREWICZ W, et al. Prog Part Nucl Phys, 2007, 59(1): 432.

[27] BLANK B, PŁOSZAJCZAK M. Rep Prog Phys, 2008, 71(4): 046301.

[28] PFÜTZNER M, KARNY M, GRIGORENKO L V, et al. Rev Mod Phys, 2012, 84(2): 567.

[29] PFÜTZNER M, MUKHA I, WANG S M. Prog Part Nucl Phy, 2023, 132: 104050.

[30] FREER M. Rep Prog Phys, 2007, 70(12): 2149.

[31] REINHARD P G. Rep Prog Phys, 1989, 52(4): 439.

[32] RING P. Prog Part Nucl Phys, 1996, 37(0): 193.

[33] VRETENAR D, AFANASJEV A V, LALAZISSIS G A, et al. Phys Rep, 2005, 409(3–4): 101.

[34] NIKŠIĆ T, VRETENAR D, RING P. Prog Part Nucl Phys, 2011, 66(3): 519.

[35] LIANG H, MENG J, ZHOU S G. Phys Rep, 2015, 570: 1.

[36] MENG J. Nucl Phys A, 1998, 635(1–2): 3.

[37] MENG J, RING P. Phys Rev Lett, 1998, 80(3): 460.

[38] MENG J, TOKI H, ZENG J Y, et al. Phys Rev C, 2002, 65(4): 041302(R).

[39] LONG W H, RING P, MENG J, et al. Phys Rev C, 2010, 81(3): 031302(R).

[40] LI L L, MENG J, RING P, et al. Phys Rev C, 2012, 85(2): 024312.

[41] ZHANG K Y, WANG D Y, ZHANG S Q. Phys Rev C, 2019, 100(3): 034312.

[42] SUN X X, ZHAO J, ZHOU S G. Nucl Phys A, 2020, 1003: 122011.

[43] YANG Z H, KUBOTA Y, CORSI A, et al. Phys Rev Lett, 2021, 126(8): 082501.

[44] SUN X X. Phys Rev C, 2021, 103(5): 054315.

[45] ZHANG K Y, PAPAKONSTANTINOU P, MUN M H, et al. Phys Rev C, 2023, 107(4): L041303.

[46] ZHANG K Y, YANG S Q, AN J L, et al. Phys Lett B, 2023, 844: 138112.

[47] SUN X X, ZHOU S G. Phys Rev C, 2021, 104(6): 064319.

[48] SUN X X, ZHOU S G. Sci Bull, 2021, 66(20): 1521.

[49] ZHANG K, CHEOUN M K, CHOI Y B, et al. Phys Rev C, 2020, 102(2): 024314.

[50] ZHANG K, CHEOUN M K, CHOI Y B, et al. At Data Nucl Data Tables, 2022, 144: 101488.

[51] PAN C, CHEOUN M K, CHOI Y B, et al. (DRHBc Mass Table Collaboration). Phys Rev C, 2022, 106(1): 014316.

[52] DOBACZEWSKI J, FLOCARD H, TREINER J. Nucl Phys A, 1984, 422(1): 103.

[53] KUCHAREK H, RING P. Z Phys A, 1991, 339(1): 23.

[54] ZHOU S G, MENG J, RING P. Phys Rev C, 2003, 68(3): 034323.

[55] SEROT B, WALECKA J. Adv Nucl Phys, 1986, 16: 1.

[56] RING P, SCHUCK P. The Nuclear Many-body Problem[M]. Berlin Heidelberg: Springer-Verlag, 1980.

[57] XIA X W, LIM Y, ZHAO P W, et al. At Data Nucl Data Tables, 2018, 121–122: 1.

[58] SCHUNCK N, EGIDO J L. Phys Rev C, 2008, 77(1): 011301.

[59] CHEN Y, LI L, LIANG H, et al. Phys Rev C, 2012, 85(6): 067301.

[60] LU X L, SUN B Y, LONG W H. Phys Rev C, 2013, 87(3): 034311.

[61] GENG J, LONG W H. Phys Rev C, 2022, 105(3): 034329.

[62] ZHANG K Y, ZHANG S Q, MENG J. Phys Rev C, 2023, 108(4): L041301.

[63] ZHANG K Y, PAN C, ZHANG S Q. Phys Rev C, 2022, 106(2): 024302.

[64] XIA X W, SHI Z. Commun Theor Phys, 2023, 75(4): 045301.

[65] XIANG Y, LUO Q, YANG S, et al. Symmetry, 2023, 15(7): 1420.

[66] BENDER M, BONCHE P, DUGUET T, et al. Phys Rev C, 2004, 69(6): 064303.

[67] YAO J M, BENDER M, HEENEN P H. Phys Rev C, 2015, 91(2): 024301.

[68] RODRÍGUEZ T R, POVES A, NOWACKI F. Phys Rev C, 2016, 93(5): 054316.

[69] HANSEN P G, JONSON B. Europhys Lett, 1987, 4(4): 409.

[70] DOBACZEWSKI J, NAZAREWICZ W, WERNER T R, et al. Phys Rev C, 1996, 53(6): 2809.

[71] LALAZISSIS G A, KÖNIG J, RING P. Phys Rev C, 1997, 55(1): 540.

[72] BAUMANN T, AMTHOR A M, BAZIN D, et al. Nature, 2007, 449(7165): 1022.

[73] TSUNODA N, OTSUKA T, TAKAYANAGI K, et al. Nature, 2020, 587(7832): 66.

[74] KONDO Y, NAKAMURA T, AOI N, et al. Phys Rev C, 2005, 71(4): 044611.

[75] DOMBRÁDI ZS, ELEKES Z, KANUNGO R, et al. Phys Lett B, 2005, 621(1): 81.

[76] COOK K J, NAKAMURA T, KONDO Y, et al. Phys Rev Lett, 2020, 124(21): 212503.

[77] KANADA-EN'YO Y, HORIUCHI H. Phys Rev C, 1995, 52(2): 647.

[78] KANADA-EN'YO Y, HORIUCHI H. Prog Theor Phys Suppl, 2001, 142: 205.

[79] LALAZISSIS G A, VRETENAR D, RING P. Eur Phys J A, 2004, 22(1): 37.

[80] LEBLOND S, MARQUÉS F M, GIBELIN J, et al. Phys Rev Lett, 2018, 121(26): 262502.

[81] SUN X X, GUO L. Phys Rev C, 2023, 107(1): L011601.

[82] TANAKA K, YAMAGUCHI T, SUZUKI T, et al. Phys Rev Lett, 2010, 104(6): 062701.

[83] KOBAYASHI N, NAKAMURA T, TOSTEVIN J A, et al. Phys Rev C, 2012, 86(5): 054604.

[84] TOGANO Y, NAKAMURA T, KONDO Y, et al. Phys Lett B, 2016, 761: 412.

[85] HORIUCHI W, SUZUKI Y. Phys Rev C, 2006, 74(3): 034311.

[86] CORAGGIO L, COVELLO A, GARGANO A, et al. Phys Rev C, 2010, 81(6): 064303.

[87] YAMASHITA M, DE CARVALHO R M, FREDERICO T, et al. Phys Lett B, 2011, 697(1): 90.

[88] ERSHOV S N, VAAGEN J S, ZHUKOV M V. Phys Rev C, 2012, 86(3): 034331.

[89] OGATA K, MYO T, FURUMOTO T, et al. Phys Rev C, 2013, 88(2): 024616.

[90] ACHARYA B, JI C, PHILLIPS D. Phys Lett B, 2013, 723: 196.

[91] KUCUK Y, TOSTEVIN J A. Phys Rev C, 2014, 89(3): 034607.

[92] HOFFMAN C R, KAY B P, SCHIFFER J P. Phys Rev C, 2014, 89(6): 061305(R).

[93] INAKURA T, HORIUCHI W, SUZUKI Y, et al. Phys Rev C, 2014, 89(6): 064316.

[94] SOUZA L A, GARRIDO E, FREDERICO T. Phys Rev C, 2016, 94(6): 064002.

[95] SUZUKI T, OTSUKA T, YUAN C, et al. Phys Lett B, 2016, 753: 199.

[96] SOUZA L, BELLOTTI F, YAMASHITA M, et al. Phys Lett B, 2016, 757: 368.

[97] NAGAHISA T, HORIUCHI W. Phys Rev C, 2018, 97(5): 054614.

[98] WANG M, HUANG W, KONDEV F, et al. Chin Phys C, 2021, 45(3): 030003.

[99] SUZUKI T, KANUNGO R, BOCHKAREV O, et al. Nucl Phys A, 1999, 658(4): 313.

[100] KANUNGO R, HORIUCHI W, HAGEN G, et al. Phys Rev Lett, 2016, 117(10): 102501.

[101] ZHONG S Y, ZHANG S S, SUN X X, et al. Sci China-Phys Mech Astron, 2022, 65(6): 262011.

[102] GENG J, NIU Y F, LONG W H. Chinese Phys C, 2023, 47(4): 044102.

[103] PEI J C, ZHANG Y N, XU F R. Phys Rev C, 2013, 87(5): 051302(R).

[104] PEI J C, KORTELAINEN M, ZHANG Y N, et al. Phys Rev C, 2014, 90(5): 051304(R).

[105] ZHANG Y N, PEI J C, XU F R. Phys Rev C, 2013, 88(5): 054305.

[106] NAKADA H, TAKAYAMA K. Phys Rev C, 2018, 98(1): 011301(R).

[107] SUN T T, QIAN L, CHEN C, et al. Phys Rev C, 2020, 101(1): 014321.

[108] QU X, ZHANG Y. Sci China Phys Mech Astron, 2019, 62(11): 112012.

[109] CAO X N, LIU Q, GUO J Y. J Phys G: Nucl Part Phys, 2018, 45(8): 085105.

[110] ZHANG S S, SMITH M S, KANG Z S, et al. Phys Lett B, 2014, 730: 30.

[111] MOLLER P, NIX J, MYERS W, et al. At Data Nucl Data Tables, 1995, 59(2): 185.

[112] MÖLLER P, SIERK A J, ICHIKAWA T, et al. At Data Nucl Data Tables, 2016, 109–110: 1.

[113] WANG N, LIU M, WU X Z. Phys Rev C, 2010, 81(4): 044322.

[114] WANG N, LIU M, WU X Z, et al. Phys Lett B, 2014, 734: 215.

[115] GORIELY S, CHAMEL N, PEARSON J M. Phys Rev C, 2013, 88(2): 024308.

[116] ZHANG K, PAN C, ZHANG S, et al. Chin Sci Bull, 2021, 66(27): 3561.

[117] GUO P, CAO X, CHENG K, et al. At Data Nucl Data Tables, 2024, 158: 101661.

[118] IN E J, PAPAKONSTANTINOU P, KIM Y, et al. Int J Mod Phys E, 2021, 30: 2150009.

[119] PAN C, ZHANG K, ZHANG S. Int J Mod Phys E, 2019, 28(09): 1950082.

[120] ZHANG K, HE X, MENG J, et al. Phys Rev C, 2021, 104(2): L021301.

[121] PAN C, ZHANG K Y, CHONG P S, et al. Phys Rev C, 2021, 104(2): 024331.

[122] HE X T, WANG C, ZHANG K Y, et al. Chin Phys C, 2021, 45(10): 101001.

[123] ZHANG X Y, NIU Z M, ZHANG W, et al. Phys Rev C, 2023, 108(2): 024310

[124] CHOI Y B, LEE C H, MUN M H, et al. Phys Rev C, 2022, 105(2): 024306.

[125] KIM S, MUN M H, CHEOUN M K, et al. Phys Rev C, 2022, 105(3): 034340.

[126] GUO P, PAN C, ZHAO Y C, et al. Phys Rev C, 2023, 108(1): 014319.

[127] SUN W, ZHANG K Y, PAN C, et al. Chin Phys C, 2022, 46(6): 064103.

[128] SUN X, MENG J. Phys Rev C, 2022, 105(4): 044312.

[129] ROBLEDO L M, RODRÍGUEZ T R, RODRÍGUEZ-GUZMÁN R R. J Phys G: Nucl Part Phys, 2019, 46(1): 013001.

[130] RODRÍGUEZ-GUZMÁN R R, EGIDO J L, ROBLEDO L M. Phys Rev C, 2004, 69(5): 054319.

[131] BENDER M, BONCHE P, HEENEN P H. Phys Rev C, 2006, 74(2): 024312.

[132] RODRÍGUEZ T R, EGIDO J L. Phys Rev Lett, 2007, 99(6): 062501.

[133] CUI J W, ZHOU X R, SCHULZE H J. Phys Rev C, 2015, 91(5): 054306.

[134] CUI J W, ZHOU X R, GUO L X, et al. Phys Rev C, 2017, 95(2): 024323.

[135] MEI H, HAGINO K, YAO J M, et al. Phys Rev C, 2018, 97(6): 064318.

[136] XIA H J, WU X Y, MEI H, et al. Sci China Phys Mech Astron, 2019, 62(4): 42011.

[137] BENDER M, HEENEN P H. Phys Rev C, 2008, 78(2): 024309.

[138] RODRÍGUEZ T R, EGIDO J L. Phys Rev C, 2010, 81(6): 064323.

[139] YAO J M, MENG J, RING P, et al. Phys Rev C, 2009, 79(4): 044312.

[140] YAO J M, MENG J, RING P, et al. Phys Rev C, 2010, 81(4): 044311.

[141] YAO J M, HAGINO K, LI Z P, et al. Phys Rev C, 2014, 89(5): 054306.

[142] EGIDO J L, BORRAJO M, RODRÍGUEZ T R. Phys Rev Lett, 2016, 116(5): 052502.

[143] YAO J M, ZHOU E F, LI Z P. Phys Rev C, 2015, 92(4): 041304(R).

[144] RODRÍGUEZ-GUZMÁN R, ROBLEDO L M, SARRIGUREN P. Phys Rev C, 2012, 86(3): 034336.

[145] RODRÍGUEZ-GUZMÁN R, HUMADI Y M, ROBLEDO L M. J Phys G: Nucl Part Phys, 2020, 48(1): 015103.

[146] MAREVIĆ P, SCHUNCK N. Phys Rev Lett, 2020, 125(10): 102504.

[147] EGIDO J L, JUNGCLAUS A. Phys Rev Lett, 2020, 125(19): 192504.

[148] EGIDO J L, JUNGCLAUS A. Phys Rev Lett, 2021, 126(19): 192501.

[149] ZHOU E, YAO J, LI Z, et al. Phys Lett B, 2016, 753: 227.

[150] WANG K, LU B. Commun Theor Phys, 2022, 74(1): 015303.

[151] RONG Y T, WU X Y, LU B N, et al. Phys Lett B, 2023, 840: 137896.

[152] MAREVIĆ P, EBRAN J P, KHAN E, et al. Phys Rev C, 2019, 99(3): 034317.

[153] ZHAO P W, LI Z P, YAO J M, et al. Phys Rev C, 2010, 82(5): 054319.

变形晕核中的形状退耦合及转动激发

孙向向 [1,2], 周善贵 [1,2,3,4,†]

(1. 中国科学院大学核科学与技术学院，北京 100049；
2. 中国科学院理论物理研究所，理论物理前沿重点实验室，北京 100190；
3. 中国科学院大学物理学院，北京 100049；
4. 北京航空航天大学彭桓武科教合作中心，北京 100191)

摘要： 随着放射性核束物理的快速发展，在远离 β 稳定线的原子核中发现或者预言了很多奇特现象，包括集团结构、壳结构演化、变形晕、变形晕核中形状退耦合等。对这些奇特核现象的研究是当前核物理的重要前沿领域。协变密度泛函理论 (CDFT) 是描述核素图上几乎所有原子核性质最成功的微观方法之一。在 CDFT 下，为了恰当地处理形变效应和奇特原子核的弱束缚特性，发展了包含连续谱的变形相对论性 Hartree-Bogoliubov 理论 (deformed relativistic Hartree-Bogoliubov theory in continuum, DRHBc)。在本文中，将总结 DRHBc 理论在奇特核结构研究中的应用以及其扩展。DRHBc 理论已用于描述硼、碳、氖、钠和镁同位素链中的变形中子晕现象，并且计算结果符合相关的实验数据。DRHBc 质量表合作组正在致力于用该理论构建考虑形变和连续谱效应的高精度原子核质量表。此外，基于 DRHBc 理论的角动量投影计算表明：在变形晕核的低激发转动态中依然存在晕现象以及形状退耦合现象。

关键词： 奇特原子核；变形晕；形状退耦合；原子核质量；转动激发；协变密度泛函理论